Two-Phase Fluid Displacement and Interfacial Instabilities Under Elastic Membranes

Talal T. Al-Housseiny, Ivan C. Christov, and Howard A. Stone

Phys. Rev. Lett. **111**, 034502 — Published 16 July 2013

DOI: 10.1103/PhysRevLett.111.034502

Two-phase fluid displacement and interfacial instabilities under elastic membranes

Talal T. Al-Housseiny,[1,*] Ivan C. Christov,[2] and Howard A. Stone[2]

[1]*Department of Chemical and Biological Engineering, Princeton University, Princeton, NJ 08544, USA*
[2]*Department of Mechanical and Aerospace Engineering, Princeton University, Princeton, NJ 08544, USA*

(Dated: May 6, 2013)

In this work, we study the elastic version of the Saffman–Taylor problem: the Hele-Shaw displacement of a viscous liquid by a gas underneath an elastic membrane. We derive the dynamics of the propagating gas-liquid interface and of the deforming membrane. Even though the displacement of a viscous liquid by a gas is susceptible to viscous fingering, the presence of the elastic boundary can lead to the suppression of the instability. We demonstrate how the mechanism of suppression is provided by surface tension at the gas-liquid interface owing to the tapered flow geometry underneath the deflected membrane. We also determine the critical conditions for the onset of the fingering instability in the presence of the elastic boundary.

PACS numbers: 47.15.gp, 47.20.Ma, 87.10.Pq

Elastohydrodynamics [1] spans a broad range of applications that involve the interaction of fluid flow and compliant boundaries. Such fluid-structure interactions are abundant in nature and technology at all scales; examples include the lateral intrusion of magma under a terrestrial crust [2, 3], blood creeping underneath the skin giving bruises their signature color, hydraulic fracturing [4] and the manufacturing of semiconductors [5]. These nonlinear systems are susceptible to interfacial instabilities when multiphase flows are involved, which inspires the present work.

In this Letter, we treat the elastic version of the Saffman–Taylor problem: the displacement of a viscous fluid by a gas underneath an elastic membrane. Motivated by a recent experimental study [6], we consider a radial flow confined between two closely spaced plates, i.e. a radial Hele-Shaw cell [7, 8], where the upper plate is an elastic sheet and the lower plate is rigid and horizontal. The cell is initially filled with a thin film of a viscous liquid, which is then displaced by a gas injected at the center of the cell. First, we consider single-phase spreading underneath an elastic membrane and show that this simpler system does not describe the experiments in [6]. Second, we study a stable (circular) interface propagating in a two-phase system and subsequently extract the dynamics of the deforming membrane. Third, we examine the stability of a gas-liquid interface in the presence of an elastic boundary. In a traditional Hele-Shaw cell with rigid plates, the interface between a viscous liquid and the injected gas is susceptible to the viscous fingering instability [8–11]. However, the presence of an elastic membrane can stabilize the gas-liquid interface [6]. We identify the mechanism for this suppression to be the tapered flow passage resulting from the deflection of the membrane, and we find the conditions under which the stabilization occurs. Thus, elastic membranes offer geometrical means to control the fingering instability [6, 12–14].

Single-phase spreading To start, let us consider the spreading of a fluid with viscosity μ under an elastic membrane with zero initial height [2]; see Fig. 1a. As the fluid is supplied at the center ($r = 0$) with a constant flow rate Q, the thin and massless elastic membrane bends axisymmetrically, rendering the dynamics dependent only on the radius r and time t. Assuming the flow to be incompressible, the continuity equation is

$$\frac{\partial h}{\partial t} + \frac{1}{r}\frac{\partial}{\partial r}\left(rhu\right) = 0\,, \tag{1}$$

where $h(r,t)$ is the height of the elastic membrane and $u(r,t)$ is the fluid's depth-averaged velocity, which for viscous flows can be described by Darcy's law [15]. Assuming that the gravitational forces acting on the fluid are much smaller than viscous forces, we have

$$u = -\frac{h^2}{12\mu}\,\frac{\partial p}{\partial r}\,. \tag{2}$$

Neglecting inertia and stretching of the membrane [15], the depth-averaged pressure in the fluid $p(r,t)$ must match the bending stress of the membrane. For small deformations, the membrane obeys linear elasticity so that $p = B\nabla^4 h$ [16], where B is the bending modulus of the membrane. Substituting (2) into (1) and using the expression for the pressure, we obtain the governing partial differential equation (PDE) for the deflection of the membrane [2]:

$$\frac{\partial h}{\partial t} = \frac{B}{12\mu}\frac{1}{r}\frac{\partial}{\partial r}\left(rh^3\frac{\partial}{\partial r}\nabla^4 h\right), \tag{3}$$

where $\nabla^4 h = \frac{1}{r}\frac{\partial}{\partial r}\left(r\frac{\partial}{\partial r}\left(\frac{1}{r}\frac{\partial}{\partial r}\left(r\frac{\partial h}{\partial r}\right)\right)\right)$ for axisymmetric shapes. The PDE (3) is subject to a global mass conservation constraint, which, for a constant rate of injection, is written as

$$2\pi\int_0^\infty h(r,t)\,r\,\mathrm{d}r = Q\,t\,. \tag{4}$$

A scaling analysis of the PDE (3) subject to the constraint (4) reveals that

$$h \sim \left(\frac{\mu}{B}\right)^{1/6} Q^{1/2}\,t^{1/3} \text{ and } r \sim \left(\frac{\mu}{B}\right)^{-1/12} Q^{1/4}\,t^{1/3}. \tag{5}$$

Thus, for steady injection of a fluid underneath an elastic membrane with zero initial height, we infer from (5) that both the extent of spreading of the fluid and the height of the membrane increase as $t^{1/3}$.

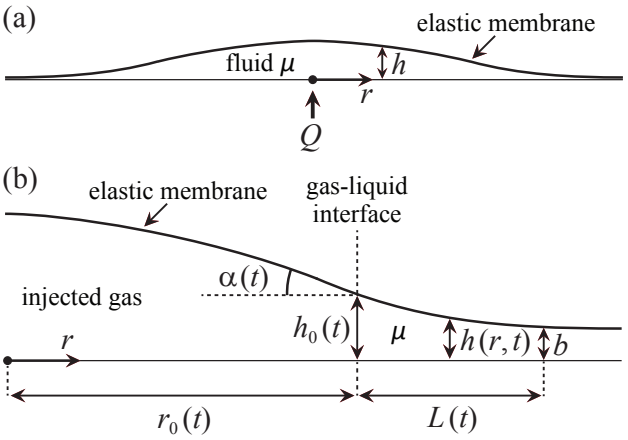

FIG. 1. (a) Single-phase spreading. Schematic of a system in which a fluid of viscosity μ is injected at a constant flow rate Q underneath a thin elastic membrane with zero initial height. (b) Two-phase displacement. Schematic of a radial Hele-Shaw cell where the bottom boundary is a rigid horizontal plate and the top boundary is a thin elastic sheet. A gas is injected at the center of the cell at a constant flow rate Q, displacing a viscous liquid of viscosity μ and deflecting the elastic membrane. The height of the membrane $h(r,t)$ is initially b and the gas-liquid interface is located at $r = r_0(t)$.

Two-phase displacement Consider now a two-phase system representative of the experiments [6]; see Fig. 1b. A Hele-Shaw cell with depth b and an elastic top boundary is initially filled with a wetting viscous liquid of viscosity μ and density ρ. At the center of the cell, a gas is injected at a constant flow rate Q displacing the viscous liquid axisymmetrically in the radial direction, while also deflecting the elastic membrane. The position and velocity of the gas-liquid interface are denoted by $r_0(t)$ and $U(t) = dr_0/dt$ respectively, and the corresponding cell height is $h(r_0(t)) = h_0(t)$. Experiments conducted in this setup revealed that the interface advances as $r_0(t) \sim t^{0.36\pm0.01}$ [6, 17], which is slightly faster than the $t^{1/3}$ dynamics of single-phase spreading (eq. (5)). Furthermore, the experiments exhibited a dependence on the initial cell depth b, which is a feature not accounted for by the single-phase analysis above. In what follows, we obtain an analytical description of the dynamics of two-phase displacements, accounting for all parameters including b.

As the gas invades the Hele-Shaw cell and deflects its upper boundary, the viscous liquid accumulates under the deformed elastic membrane forming a moving front ahead of the interface; see Fig. 1b. Our model relies on the idea that the dynamics are set by this region of accumulation, beyond which the elastic membrane is undeformed. Thus, the moving front is assumed to have a finite extent $L(t)$: $h\big(r \geq r_0(t)+L(t)\big) = b$. As the interface propagates radially, the volume of liquid accumulating under the moving front increases, and it must be equal to the volume of liquid displaced by the gas. Assuming a sharp gas-liquid interface, i.e. neglecting residual wetting films trailing behind the moving interface, mass conservation dictates that

$$2\pi \int_{r_0(t)}^{r_0(t)+L(t)} \big(h(r,t) - b\big) r \, \mathrm{d}r = \pi \big(r_0(t)\big)^2 b. \qquad (6)$$

In the moving front, the deformation of the membrane is small, so we can neglect stretching strains [15, 18]. In addition, gravitational forces acting on the displaced fluid are negligible in comparison to viscous forces; in the experiments $\rho g h_0^3 \,/\, 12\mu U L \ll 1$, where g is the gravitational acceleration.

To obtain the deflection $h(r,t)$ of the membrane over the moving front, we must add the advection velocity $U(t)$ to the right-hand side of (2). Then, the two-phase version of (3) is

$$\frac{\partial h}{\partial t} + \frac{dr_0}{dt}\frac{1}{r}\frac{\partial}{\partial r}(rh) = \frac{B}{12\mu}\frac{1}{r}\frac{\partial}{\partial r}\left(rh^3\frac{\partial}{\partial r}\nabla^4 h\right), \qquad (7)$$

subject to the boundary conditions:

$$h|_{r=r_0} = h_0(t), \;\; h|_{r=r_0+L} = 0, \;\; h^3\frac{\partial}{\partial r}\nabla^4 h\bigg|_{r=r_0+L} = 0. \qquad (8)$$

The third condition in (8) enforces no flux at the leading edge of the moving front. Moreover, observe that (8) neglects terms of $O(b/h_0)$, which is small in the experiments [6, 17].

The last boundary condition [19] is imposed on the slope $\alpha(t)$ of the membrane at $r = r_0(t)$; see Fig. 1b. The slope $\alpha(t)$ can be related to other parameters based on a geometric analysis [20], which assumes a slender membrane $\alpha \ll 1$. Neglecting compression in the gas phase, i.e. the resistance to the bending of the thin membrane is much smaller than the resistance to the compression of the gas, the volume occupied by the gas under the slender membrane is $Q\,t$, so that

$$\alpha(t) = \frac{\partial h}{\partial r}\bigg|_{r=r_0} = -\frac{3}{\pi}\frac{Q\,t}{r_0^3} + O\left(\frac{h_0}{r_0}\right). \qquad (9)$$

Note that (9) relates $\alpha(t)$ to the interface position $r_0(t)$, which we later determine from the physical balances of the system.

As the interface propagates radially, the elastic membrane is deflected and the volume of the moving front increases. As a result, $h_0(t)$, $r_0(t)$ and $L(t)$ increase such that $\varepsilon(t) = L(t)/r_0(t) \ll 1$ decreases in time, approaching zero. In the slope condition (9), we can neglect terms of $O(h_0/r_0)$ since $h_0/r_0 = \varepsilon h_0/L$ while $\alpha = O(h_0/L)$.

A local scaling analysis of (7) shows that, for long times, $\partial h/\partial t$ is $O(\varepsilon)$ in comparison to the convective term. Thus, the dominant balance between the convective and elastic terms yields a quasi-steady moving front [21] of the form

$$h(r,t) = h_0(t)(1-x)^{5/3}, \qquad x = \frac{r - r_0(t)}{L(t)}. \qquad (10)$$

Since we neglected terms of $O(b/h_0)$ in (8), our model (10) does not capture $O(b/h_0)$ distortions of the elastic membrane. The speed of the front is obtained by first substituting (10) into (7). Neglecting terms of $O(\varepsilon)$ and $O\left((\mu L^6/Bh_0^4)dh_0/dt\right)$, we then find that the front is traveling at a speed

$$\frac{dr_0}{dt} = \frac{280}{243}\frac{B}{12\mu}\frac{h_0^3}{L^5}. \qquad (11)$$

Now, we substitute (10) into the conservation constraint (6) and the slope condition (9). To the leading order, we obtain

$$L\,h_0 = \frac{4}{3}\,b\,r_0\,, \tag{12}$$

$$\frac{h_0}{L} = \frac{9}{5\pi}\,\frac{Q\,t}{r_0^3}\,. \tag{13}$$

Solving the system (11)–(13) for the three unknowns $r_0(t)$, $h_0(t)$ and $L(t)$, we find the power laws:

$$r_0(t) = C_r \left(\frac{B\,Q^4}{\mu\,b}\right)^{1/14} t^{5/14},$$

$$\text{where} \quad C_r = \left(\frac{1323}{625\,\pi^4}\right)^{1/14} \approx 0.76\,, \tag{14a}$$

$$h_0(t) = C_h \left(\frac{\mu\,b^8\,Q^3}{B}\right)^{1/14} t^{1/7},$$

$$\text{where} \quad C_h = 2\left(\frac{81}{6125\,\pi^3}\right)^{1/14} \approx 1.15\,, \tag{14b}$$

$$L(t) = C_L \left(\frac{B^2\,b^5\,Q}{\mu^2}\right)^{1/14} t^{3/14},$$

$$\text{where} \quad C_L = \frac{2}{3}\left(\frac{2401}{15\,\pi}\right)^{1/14} \approx 0.88\,. \tag{14c}$$

The self-similar dynamics described by (14) are weakly sensitive to the physical properties and parameters of the system. Using (14), we can show that the neglected quantities $\varepsilon = L/r_0$, b/h_0 and $(\mu L^6/Bh_0^4)dh_0/dt$ all scale identically:

$$\varepsilon\,,\ \frac{b}{h_0}\,,\ \frac{\mu L^6}{Bh_0^4}\frac{dh_0}{dt} \sim \left(\frac{B\,b^6}{\mu\,Q^3}\right)^{1/14} t^{-1/7} \simeq O(10^{-1}) \tag{15}$$

for typical times in [6], and decay to zero as $t \to \infty$.

Next, we compare our theoretical results, which have no adjustable parameters, to the experimental findings [6, 17]. In particular, we predict from (14a) that a stable (circular) interface advances under an elastic membrane as $r_0 \sim t^{5/14}$, which is in excellent agreement with the $t^{0.36}$ scaling observed experimentally [6, 17]. Fig. 2 shows that, for two disparate sets of conditions, our asymptotic analysis captures the dynamics of the two-phase system. This agreement supports our hypothesis that the dynamics are set by the liquid accumulating under the moving front. We note that both the relative deviation of the prefactor C_r and the spread of the experimental data are $O(\varepsilon)$ (see [20]).

We can extend our analysis, in which we consider a gas displacing a viscous liquid, to an injected fluid of finite viscosity μ_i if the viscous forces in the injected fluid ($\sim \mu_i U r_0^2/h_0$) are much smaller than the viscous forces in the displaced fluid ($\sim \mu U L r_0/h_0$). That is, our asymptotic analysis is valid if $\mu_i/\mu \ll \varepsilon$. This condition is met in [6], where $\mu_i/\mu \simeq 10^{-5}$ and $\varepsilon \simeq 10^{-1}$. We expect our results to hold, for instance, if the injected fluid is water, for which $\mu_i/\mu \simeq 10^{-3}$. In such a scenario, gravitational forces are still negligible since water and the displaced vicous liquid have comparable densities.

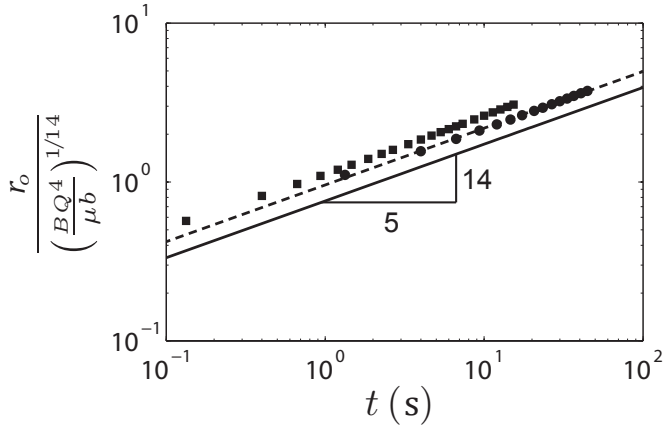

FIG. 2. Propagation of the gas-liquid interface. Comparison between our prediction (—) in (14a) and the experiments in [6], which were conducted using a liquid of viscosity $\mu = 1.04$ kg m^{-1}s^{-1} and a membrane with bending modulus B. The initial membrane height is b, and then, nitrogen gas is injected at a constant flow rate Q. (●) $Q = 55$ mL min^{-1}, $B = 1.46 \times 10^{-1}$ N mm and $b = 0.56$ mm. (■) $Q = 300$ mL min^{-1}, $B = 2.81 \times 10^{-2}$ N mm and $b = 0.79$ mm. The dashed line is (14a) with the prefactor is adjusted to be $1.25 \times C_r$. The units of the vertical axis are s$^{5/14}$.

Inhibiting viscous fingering In a Hele-Shaw cell with rigid boundaries, the interface between a gas injected at a constant rate and a displaced viscous liquid is unstable owing to the viscous fingering instability [7, 8]. In contrast, if the upper boundary of the cell is an elastic membrane, the gas-liquid interface can be stabilized at low flow rates [6]. Next, we explain this finding and determine the critical injection rate.

Since displacement in the two-phase system is flow-rate-controlled, the surface tension γ at the gas-liquid interface does not contribute to the dynamics of a stable (circular) interface propagating underneath an elastic membrane. However, surface tension forces are instrumental in determining the stability of the interface. To investigate interfacial instabilities, it is important to examine the shape of the flow passage in the neighborhood of the interface [12, 14]. To this end, we calculate the slope $\alpha(t)$ of the elastic membrane at the interface by substituting (10), (14b) and (14c) into the definition of the slope $\alpha = \frac{\partial h}{\partial r}\big|_{r=r_0}$. We find that

$$\alpha(t) = -\,C_\alpha \left(\frac{\mu^3\,b^3\,Q^2}{B^3}\right)^{1/14} t^{-1/14}, \tag{16}$$

where $C_\alpha = \frac{5}{3}\frac{C_h}{C_L} \approx 2.17$. The inclination of the membrane varies very slowly in time and, in particular, it changes much more slowly than the position of the interface.

The previous disparity, between the change of membrane inclination ($d\alpha/dt \sim t^{-15/14}$) and the rate of fluid displacement ($dr_0/dt \sim t^{-9/14}$), suggests that we must first under-

stand the stability of an interface propagating in the fixed (static) tapered geometry induced by the deflected membrane; see Fig. 1b. Recently, Al-Housseiny *et al.* [12] demonstrated the control of viscous fingering in the presence of a taper. For a radially tapered Hele-Shaw cell, they derived a stability criterion [13] that predicts that the interface between a gas and a perfectly wetting viscous liquid is stable if

$$1 + \frac{2\alpha + h_0^2/r_0^2}{Ca} < 0\,, \tag{17}$$

where $Ca = 12\mu U/\gamma$ is a characteristic capillary number for the Hele-Shaw configuration. Here, since unstable modes grow exponentially, the elastic membrane is stationary at the time scale of the instability. The mean speed of the interface is then given by $U(t) = Q/(2\pi r_0 h_0)$.

In the absence of a taper, i.e. for $\alpha = 0$, the inequality in (17) cannot be satisfied, and a gas propagating into a wetting liquid always yields, for long times, an unstable interface for a constant injection rate [7, 8]. As in (9), $h_0^2/r_0^2 \ll \alpha$. Thus, the stability condition in (17) reduces to $Ca < 2|\alpha|$ for long times. As a result, there exists a critical displacement speed below which the fingering instability is suppressed [12, 13]. We can rewrite $Ca < 2|\alpha|$ using (14a), (14b) and (16) as

$$r_c = C_r \left(\frac{3}{\pi}\,\frac{1}{C_r C_h C_\alpha}\,\frac{\mu}{\gamma b^{1/2}}\right)^{5/6} \left(\frac{B}{\mu\, b}\right)^{1/4} Q^{7/12}, \tag{18}$$

where r_c is the critical radius at which the stably propagating gas-liquid interface is predicted to transition to an unstable state. Therefore, if we tune the system parameters such that the radius of fluid displacement is always smaller than r_c, then the interfacial instability will not be manifested.

Alternatively, for a stable interface located at a given radius R, we can determine a critical flow rate Q_c above which the interface becomes unstable. Rearranging (18), we find

$$Q_c = C_Q\,\frac{\gamma R}{\mu}\left(\frac{\gamma^3\, R^5\, b^8}{B^3}\right)^{1/7}, \tag{19}$$

where $C_Q = \left(\frac{\pi}{3} C_h C_\alpha\right)^{10/7} C_r^{-2/7} \approx 4.26$. Thus, we infer that $Q_c \sim B^{-3/7}$. This dependence is supported by the experimental findings in [6] as shown in Fig. 3. Hence, the mechanism we have identified, based on the taper caused by the deflection of the membrane, captures the influence of the elastic boundary on the onset of the viscous fingering instability. We note that the limit $B \to \infty$ corresponds to the classical system with rigid parallel plates, in which the interface is always unstable at late times for a constant rate of injection.

Conclusion We studied the displacement of a viscous liquid by a gas in a radial Hele-Shaw cell with an elastic top boundary. We found that the dynamics of this two-phase system are predominantly set by the viscous liquid that accumulates ahead of the interface. Furthermore, the compliance of the membrane can facilitate the inhibition of the classical viscous fingering instability. As the gas is injected at the center of the elastic cell, the membrane is deflected forming a tapered geometry over the gas-liquid interface. This taper, rather than bending stresses alone [6], is the underlying geometric mechanism responsible for the suppression of the instability. The interface remains stable since the tip of any developing finger experiences higher capillary resistance than the lagging parts of the finger owing to the tapered geometry [12, 14]. A number of studies have previously focused on a variety of injection schemes to control viscous fingering [23–26]. In contrast, elastic membranes present a simple geometrical approach.

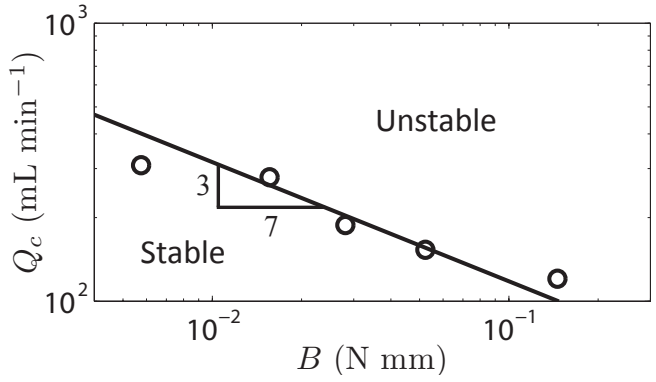

FIG. 3. The influence of the bending modulus on the onset of viscous fingering. Comparison between our scaling for the critical flow rate (19) and the experimental results (○) in [6]. To vary the bending modulus B in the experiments, membranes of different thicknesses were used. The critical flow rate Q_c is the minimum gas flow rate required to initiate an interfacial instability at $R = 5$ cm. The initial height of the elastic membrane is $b = 0.56$ mm. The viscosity and the surface tension of the displaced wetting liquid are $\mu = 1.04$ kg m^{-1}s^{-1} and $\gamma = 22$ mN m^{-1}, respectively. The solid line represents (19) with the prefactor adjusted to be $1.7 \times C_Q$. This offset in the prefactor is expected due to the cumulative discrepancies resulting from the asymptotic approximation (15) and from neglecting the effect of the wetting film [12, 22] on the stability threshold (17).

The authors thank A. Juel and D. Pihler-Puzović for sharing their data, the referees for valuable feedback, G. M. Homsy, P. A. Tsai and J. R. Lister for discussions. H. A. Stone is supported by the National Science Foundation (NSF) under Grant No. CBET-1132835. I. C. Christov is supported by the NSF under Grant No. DMS-1104047. T. T. Al-Housseiny is supported by the NSF Graduate Research Fellowship under Grant No. DGE-0646086.

* Electronic address: talal@princeton.edu

[1] R. Gohar, *Elastohydrodynamics* (Imperial College Press, London, 2001).
[2] C. Michaut, J. Geophys. Res. **116**, B05205 (2011).
[3] M. Khomenko, *Viscous Fluid Instabilities Under an Elastic Sheet* (Master Thesis, The University of British Columbia, 2010).
[4] A. A. Savitski and E. Detournay, Int. J. Solids Structures **39**, 6311 (2002).
[5] J. R. King, SIAM J. Appl. Math. **49**, 264 (1989).

[6] D. Pihler-Puzović, P. Illien, M. Heil, and A. Juel, Phys. Rev. Lett. **108**, 074502 (2012).
[7] L. Paterson, J. Fluid Mech. **113**, 513 (1981).
[8] G. M. Homsy, Annu. Rev. Fluid Mech. **19**, 271 (1987).
[9] S. Hill, Chem. Eng. Sci. **1**, 247 (1952).
[10] P. G. Saffman and G. I. Taylor, Proc. R. Soc. Lond. A **245**, 312 (1958).
[11] R. L. Chuoke, P. van der Meurs, and C. van der Poel, Trans. AIME **216**, 188 (1959).
[12] T. T. Al-Housseiny, P. A. Tsai, and H. A. Stone, Nature Phys. **8**, 747 (2012).
[13] T. T. Al-Housseiny and H. A. Stone (Submitted).
[14] K. J. Ruschak, Annu. Rev. Fluid Mech. **17**, 65 (1985).
[15] A. E. Hosoi and L. Mahadevan, Phys. Rev. Lett. **93**, 137802 (2004).
[16] L. D. Landau and E. M. Lifshitz, *Theory of Elasticity* (Pergamon Press, Oxford, 1970).
[17] P. Illien, *Suppression of Viscous Fingering Under Elastic Membranes* (Stage de recherche M1, Ecole Normale Supérieure, 2011).
[18] J. Chopin, D. Vella, and A. Boudaoud, Proc. R. Soc. A **464**, 2887 (2008).
[19] The nonlinear system (6)–(8) is underspecified. However, the solution branch (10) is singly underspecified and, hence, (9) is the last boundary condition needed [21].
[20] Supplementary materials [INSERT].
[21] J. C. Flitton and J. R. King, Eur. J. Appl. Math. **15**, 713 (2004).
[22] C.-W. Park and G. M. Homsy, J. Fluid Mech. **139**, 291 (1984).
[23] S. S. S. Cardoso and A. W. Woods, J. Fluid Mech. **289**, 351 (1995).
[24] S. Li, J. S. Lowengrub, J. Fontana, and P. Palffy-Muhoray, Phys. Rev. Lett. **102**, 174501 (2009).
[25] E. O. Dias, F. Parisio, and J. A. Miranda, Phys. Rev. E **82**, 067301 (2010).
[26] E. O. Dias, E. Alvarez-Lacalle, M. S. Carvalho, and J. A. Miranda, Phys. Rev. Lett. **109**, 144502 (2012).